

IS MERCERIZATION THE ONLY FACTOR FOR (PARTIAL) POLYMORPHIC TRANSITION OF CELLULOSE I TO CELLULOSE II IN CELLULOSE NANOCRYSTALS?

TESFAYE GABRIEL,* ANTENEH BELETE,* GERD HAUSE,**
REINHARD H.H. NEUBERT***,**** and TSI GE BRE-MARIAM*

*Department of Pharmaceutics and Social Pharmacy, School of Pharmacy, College of Health Sciences, Addis Ababa University, P.O. Box 1176, Addis Ababa, Ethiopia

**Microscopy Unit, Biocenter, Martin Luther University, Halle-Wittenberg, Halle (Saale), Germany

***Department of Pharmaceutical Technology and Biopharmaceutics, Institute of Pharmacy, Martin Luther University Halle-Wittenberg, 06120 Halle (Saale), Germany

****Institute of Applied Dermatopharmacy, Martin Luther University Halle-Wittenberg, 06120 Halle (Saale), Germany

✉ Corresponding author: Tsigé Gebre-Mariam, tsige.gmariam@aau.edu.et

Received February 4, 2022

The present study aims to investigate the influence of factors such as the source of cellulose and cellulose extraction and acid hydrolysis conditions on the partial polymorphic transition of Cellulose I to the allomorphic form Cellulose II in cellulose nanocrystals (CNCs). CNCs were obtained from cellulose fibers extracted from four agro-industrial residues in Ethiopia: *teff* straw (TS), *enset* fiber (EF), sugarcane bagasse (SB) and coffee hull (CH). The cellulose fibers were extracted under chlorine-free extraction conditions, comprising alkaline pretreatment (with 17.5% (w/v) sodium hydroxide), then hydrolyzed with 64% (w/w) sulfuric acid to synthesize the CNCs. The as-obtained CNCs were characterized with X-ray diffraction (XRD), Attenuated total reflection-Fourier transform infrared (ATR-FTIR) spectroscopy, thermogravimetric analysis (TGA), and transmission electron microscopy (TEM). The XRD results revealed the CNCs isolated from cellulose fibers of EF and SB contained Cellulose I and II allomorphs like their cellulose precursors, but no Cellulose II was found in CH-CNCs. Morphological and dimensional studies of the CNCs by TEM showed shorter needle-shaped nanoscale structures. Higher alkaline conditions, with 17.5% sodium hydroxide, might not necessarily contribute to the polymorphic transition in lignocellulosic materials with higher lignin content, as evidenced in CH. Generally, the formation of Cellulose I and II allomorphs in the as-obtained CNCs was dependent on the cellulose source and cellulose extraction conditions, and less influenced by sulfuric acid hydrolysis.

Keywords: cellulose nanocrystals, cellulose I and II allomorphs, crystallinity, polymorphic transition

INTRODUCTION

Cellulose, a homopolymer with a linear β -(1 \rightarrow 4)-linked glucan structure, is the most abundant polysaccharide produced in nature.^{1,2} Woody plants and cotton are the major conventional sources of cellulose. Recently, different agricultural wastes, such as wheat straw, fibers of curaua, ramie, kenaf, jute, sisal and buti, and passion fruit peels, sunflower stalks, *etc.* are considered as potential sources of cellulose.¹⁻⁴ Other sources of cellulose include algae, marine creatures (tunicates), and bacteria.² Cellulose exists in different polymorphs (I_{α} , I_{β} , II, III₁, III₁₁, IV₁ and IV₁₁), and naturally occurs as either

Cellulose I_{α} or I_{β} . The Cellulose I_{β} (monoclinic) crystalline plane is usually present in higher plants, while Cellulose I_{α} (triclinic) exists in algae, tunicates and bacteria. Cellulose II, which comprises antiparallel chains, can be prepared from Cellulose I by regeneration or mercerization with NaOH. Both cellulose chains of I_{α} and I_{β} adopt parallel configurations without intersheet hydrogen bonding. The crystal lattice gradually changes from Cellulose I to Cellulose II at higher alkaline concentration, and the degree of polymerisation gradually decreases.^{2,3,5} In contrast to Cellulose I, Cellulose II has a more stable

structure, which makes it preferable for various applications.⁶

Cellulose nanocrystals (CNCs), also known as nanocrystalline cellulose or cellulose nanowhiskers, are unique biopolymeric materials with nanometer size and needle-like crystal structure. CNCs are produced from plant sources with a diameter of 5-20 nm and 100-500 nm in length, mainly by heat controlled acid hydrolysis, followed by mechanical treatment.^{3,4,7,8} In the acid hydrolysis process, the amorphous regions in the cellulose are removed as they undergo hydrolytic cleavage, which is promoted by hydronium ions, with the release of the individual crystallites.⁹

The CNCs usually retain Cellulose I allomorph after acid hydrolysis of disordered regions of Cellulose I materials. Cellulose II nanocrystals (CNCs-II) are usually produced from acid hydrolysis of mercerized cellulose. Additionally, CNCs-II are also prepared from Cellulose I sources under controlled reaction conditions, such as mercerization conditions and acid hydrolysis time.¹⁰ There are also reports indicating formation of CNCs-II from Cellulose I nanocrystals (CNCs-I), mercerizing the latter ones.¹¹ Cellulose I and II nanocrystal polymorphs are different in morphology, crystal structure, self-assembling structure, and performances of their derived composites for different industrial applications.¹⁰ There are a few studies that focus on the influence of preparation conditions of CNCs on polymorphic transformation of the nanocrystals.^{6,10,12}

In this study, the influence of factors such as source of cellulose, cellulose extraction and acid hydrolysis conditions was investigated on the partial polymorphic transition of cellulose to form Cellulose I and II allomorphs. Accordingly, four different lignocellulosic materials: *teff* straw (TS), *enset* fiber (EF), sugarcane bagasse (SB) and coffee hull (CH), were considered in the current study.

TS is a by-product of one of the most common staple plants, *Teff* (*Eragrostis tef* (Zuccagni) Trotter), in Ethiopia.^{13,14} EF is a by-product of *kocho*, a common local food in South and South West Ethiopia obtained from *Enset* plant (*Ensete ventricosum* (Welw.) Cheesman).^{15,16} Sugar industries generate large quantities of SB as a by-product after sucrose extraction and bioethanol production.¹⁷ Ethiopia, among the top five coffee producers in the world, is the place of origin (Kaffa province) of *Coffee arabica*, which accounts for 65%-70% of the world's coffee

production, followed by *Coffee canephora* Pierre (Robusta). Coffee is among the most popular beverages on Earth.^{18,19} CH is an agro-industrial residue available in huge quantities in coffee processing enterprises across Ethiopia, causing a significant environmental burden on the government as well as on coffee processing enterprises.²⁰

EXPERIMENTAL

Materials

Brown TS, EF, SB and CH were collected from different parts of Ethiopia.²⁰ Sodium hydroxide 97% (HiMedia, Mumbai, India), sulfuric acid 97% (BDH, England), formic acid (98%) (Central Drug House (P) Ltd. New Delhi, India), commercial cellulose (CC) (LOBA CHEMIE-Laboratory, glacial acetic acid (Riedel-de Haën), India), and hydrogen peroxide 30% (CARLO ERBA reagents, France) were used as received.

Cellulose extraction

Cellulose fibers were extracted from the four agro-industrial by-products, following a three-stage treatment according to our previous method reported elsewhere.²⁰ Briefly, the plant by-products were treated with 17.5% NaOH at 1/10 (w/v) solid/liquid ratio of dry material on a water bath at 90 °C for 1.5 h. The cooking by-products were filtered and washed repeatedly with hot distilled water. The pulps were further treated with a mixture of 20% formic acid (FA)/20% acetic acid (AA)/7.5% H₂O₂ (2:1:2) solution on water bath at 90 °C for 1.5 h, at a pulp to liquor ratio of 1:10 with continuous washing with hot water. Finally, the pulps were bleached with 7.5% H₂O₂ in alkaline media of 4% NaOH at 1:10 fiber ratio, first at room temperature for 30 min, then on the water bath at 70 °C for 30 min. Finally, the pulps were washed continuously with hot distilled water to remove residual lignin, and dried in an oven (Kottermann® 2711, Germany) for 24 h at 60 °C. The extracted cellulose fibers were designated as -Cel.

Isolation of CNCs

CNCs were obtained following a method we used previously.²¹ Accordingly, cellulose fibers extracted from the four plant by-products were hydrolyzed with 64% wt/wt sulphuric acid (1:20 g/mL) at 45 °C for 30 min under vigorous stirring. The resulting mixture was immediately diluted 10-fold with cold water, and centrifuged continuously (Beckman Coulter Avanti J-20 XP Centrifuge, USA) for each 10 min at 9,000 rpm until a cloudy suspension was formed. The hydrolyzed suspension was then dialyzed through dialysis sacks (avg. flat width 35 mm, MWCO 12,000 Da, Sigma-Aldrich, USA) against distilled water for 5 days. Finally, the suspension was homogenized by a disperser type Ultra-Turrax (Janke and Kunkel IKA-

Labortechnik, Ultra-Turrax T50) for 5 min at 10,000 rpm twice and sonicated (Bandelin SONOREX Digital 10P, Sigma-Aldrich) for 5 min. The aqueous suspension thus obtained was lyophilized (Martin Christ Gefrietrocknungsanlagen GmbH, CHRIST, An der Unteren Söse 50, 37520 Osterode am Harz, Germany). The yields of CNCs were estimated gravimetrically, considering the initial weight of the extracted celluloses. For comparison purposes, CNCs were also isolated from commercial cellulose (CC), as well as cellulose fibers extracted from the four plant materials using 5% NaOH in the pretreatment stage of cellulose extraction according to our previous study,²¹ and followed by similar acid hydrolysis conditions. The CNCs obtained from CC and the cellulose fibers were designated as CC-NCs and CNCs-5%, respectively.

Characterization of celluloses and CNCs

Attenuated total reflection (ATR)-Fourier-transform infrared (FTIR) spectroscopy studies

The FTIR spectra of the CNCs and cellulose precursors were recorded in the range from 4000 to 450 cm^{-1} using a PerkinElmer ATR-FTIR spectrometer (TWO DTGS, Llantrisant, UK), without further sample preparation.

X-ray diffraction (XRD)

The crystallinity of as-obtained CNCs and cellulose precursors was determined by an XRD-7000 X-ray Diffractometer MAXima (SHIMADZU Corporation, Japan) at 40 kV, 30 mA with monochromatic Cu-K α radiation, typically with scan speed of 3.00 $^{\circ}/\text{min}$ and sampling pitch of 0.02 $^{\circ}$. Data acquired were plotted in Origin Pro 8.5.1 in a 2 θ scale from 10 to 40.

The crystalline indices (CrIs) or the degree of crystallization (DoC) of the samples were calculated following the three approaches^{1,21-24} below:

a) the equation of Segal *et al.* (empirical method) also called peak height method:²²

$$CrI = \frac{(I_{200} - I_{am})}{I_{200}} \times 100\% \quad (1)$$

where I_{200} is the maximum intensity at the plane; and I_{am} is the intensity peak of the amorphous region, at 2 θ approximately 18 $^{\circ}$.

b) the equation of Hermans *et al.* (peak deconvolution method).^{1,21}

$$CrI = \frac{A_{cry}}{A_{total}} \times 100\% \quad (2)$$

where A_{cry} is the sum of crystalline peak areas; and A_{total} is the total area under the diffractograms.

c) the equation of Zhang *et al.*:²⁴

$$DoC = n \frac{I_k}{I_0} \times 100\%; n = 0.75 \quad (3)$$

where I_0 shows the intensities of the maximum diffraction from the baseline of the X-ray pattern and I_k indicates the intensity at the base level subtracted from this value I_0 . So, I_0 shows intensity at the 200 plane;

and I_k is obtained by subtracting intensity at the amorphous region from intensity at the 200 reflection.

Additionally, the extent of conversion of Cellulose I to Cellulose I_I in crystalline areas was derived from the equations indicated below:²⁴⁻²⁶

$$I_r = \frac{2I_{II}}{I_I + 2I_{II}} \quad (4)$$

where I_r is relative intensity number; I_I and I_{II} ($I_I + I_{II} = 1.0$) are the estimated intensity ratios of diffraction peaks with Miller indices of (110) and (1 $\bar{1}$ 0) of Cellulose I to that of (110) Cellulose I_I. I_r is defined as zero for pure native cellulose and one for completely mercerized cellulose, intermediate values of I_r indicating partially mercerized cellulose. The intensity of I_{II} is estimated from diffraction peak (110) on C_{II} and I_I arises from lattice planes (110) and (1 $\bar{1}$ 0) on C_I . I_I can be interpreted as the sum of intensities $I_{14.7} + I_{16.1}$ and I_{II} corresponds to the intensity $I_{12.0}$, then the equation is analogous to Equation (5).

The percentage of the Cellulose II form in the crystalline aggregation, equivalent to I_r , according to literature described elsewhere,^{24,25} was estimated from Equation 5:

$$C_{II} = \frac{I_{12.0}}{I_{12.0} + 0.5(I_{14.7} + I_{16.1})} \quad (5)$$

where $I_{12.0}$, $I_{14.7}$ and $I_{16.1}$ represent the intensities of diffraction peaks around 12.0, 14.7 and 16.1 (2 θ), respectively.

The percentage of Cellulose II in the samples is calculated according to Equation 6:

$$X_{II} = DoC * C_{II} \quad (6)$$

The percentage of Cellulose I in the samples is, therefore given by:

$$X_I = DoC * (1 - C_{II}) \quad (7)$$

After deconvolution of the respective XRD diffractograms following the Gaussian profile, parameters such as d-spacings (d), apparent crystallite size or thickness for the 200 plane (τ_{200}), the proportion of crystallite interior chains for the 200 plane (X_{200}), fractional variation in the plane spacing for the 200 plane ($\Delta d/d$)₂₀₀, and Z-values were obtained from equations described below.^{1,21,27,28}

The d-spacings were calculated using Bragg's equation:^{1,21}

$$d = \frac{\lambda}{2\sin\theta} \quad (8)$$

where λ is the wavelength of the incident X-rays, d is the interplanar spacing of the crystal and θ is the angle of incidence.

The average crystallite sizes for the 200 plane were estimated from the XRD patterns by Scherrer's equation:²⁷

$$\tau_{200} = \frac{\kappa\lambda}{\beta\cos\theta} \quad (9)$$

where τ_{200} is the average crystallite size for the 200-lattice plane, κ is the correction factor and usually taken to be 0.94, λ is the radiation wavelength (0.1542 nm), θ is the diffraction angle corresponding to 200-

lattice plane and β is the peak width at half maximum intensity.

The proportion of crystallite interior chains (X) was obtained from Equation (10).^{27,28}

$$X_{200} = \frac{(\tau - 2h)^2}{\tau^2} \quad (10)$$

where τ is the apparent crystallite size for the reflection of lattice plane (200), and $h = 0.57$ nm is the layer thickness of the surface chain.

Also, the fractional variation in the plane spacing $\Delta d/d$ for the 200-lattice plane was calculated following Equation (11).^{21,28}

$$\left| \frac{\Delta d}{d} \right|_{200} = \frac{\beta}{2\tau \sin \theta} \quad (11)$$

The Z -value indicates whether cellulose is I_α or I_β . The function that discriminates between I_α or I_β is given by Equation (12).^{1,21}

$$Z = 1693d_1 - 902d_2 - 549 \quad (12)$$

where d_1 is the d -spacing of the (110) peak and d_2 is the d -spacing of the (100) peak. $Z > 0$ indicates I_α ; while $Z < 0$ indicates the I_β dominant type.

Transmission electron microscopy (TEM)

A droplet of the diluted CNC suspension of 0.05% (w/v) was sonicated and deposited on a formvar-coated copper grid. The specimen was negatively stained with 2% (w/v) uranyl acetate or a 1% (w/v) phosphotungstic acid solution and dried at room temperature. The CNC samples were observed with a LIBRA 120 PLUS TEM (Carl Zeiss Microscopy, Jena, Germany) operating at 120 kV. Images were taken with a BM-2k-120 Dual-Speed on axis SSCCD-camera (TRS, Moorenweis, Germany). ImageJ was used to estimate the average length, diameter and aspect ratio, the ratio of the length to the diameter, of the respective CNCs isolated from each plant material.

Thermogravimetric analysis (TGA)

The thermal properties of the CNCs and cellulose precursors were examined with a TGA/DTG (Differential Thermo Gravimetry)-60H (SHIMADZU Corporation, Japan). The samples were heated from room temperature to 700 °C, at a heating rate of 10 °C/min and a nitrogen gas flow rate of 60 mL/min.

Statistical analysis

All data presented are mean \pm standard deviation (SD) of triplicate determinations, and were analyzed using OriginPro 8.5.1 (OriginLab Corporation, MA, USA) and Excel 2016. P value of less than 0.05 was considered to be significant difference, and Tukey's test for one-way analysis of variance (ANOVA) was applied as necessary.

RESULTS AND DISCUSSION

Cellulose extraction, CNCs isolation conditions and yield

During the process of isolation of CNCs, white gel-like materials from TS, EF and SB cellulose

fibers were obtained after hydrolysis followed by centrifugation. However, the color of the material obtained from CH cellulose was yellowish black, which may indicate carbonization during the acid hydrolysis process or the presence of high lignin in the extracted cellulose (Table 1). It has been reported elsewhere that the yellowish color of CNCs could be due to carbonization of cellulose during hydrolysis and/or the presence of residual organic substrates, including lignin and hexenuronic groups.²⁹ The CH had the highest lignin content both in the untreated material and the as-extracted cellulose²⁰ (Table 1). Additionally, the formation of colored low-molecular furan-type compounds or carbonyl groups in the cellulose chains is also the result of cellulose degradation.³⁰ The highest CNCs yield was obtained from TS cellulose (56.3%), and the least from CH cellulose (30.0%). The yields of EF-CNCs and SB-CNCs were 54.7% and 42.0%, respectively. With respect to the untreated plant materials, EF-CNCs (~33%) had the highest CNCs yield and CH-CNCs the least (~11%) (Table 1).

Crystallinity studies

From the XRD patterns (Fig. 1), the CNCs isolated from EF and SB cellulose displayed the co-existence of Cellulose I and Cellulose II, similarly to their cellulose precursors. The partial conversion of Cellulose I to Cellulose II both in the cellulose fibers and the respective CNCs obtained EF and SB was confirmed by the presence of sharp diffraction peaks around 12.0°, 20.0° and 22.0° 2θ , for the plane indices of (110), (110) and (200), respectively, which were assigned to Cellulose II.³¹⁻³³ Additionally, the appearance of a doublet in the main peak around 22° 2θ also confirmed the CNCs from EF and SB cellulose contained Cellulose II type, unlike the CNCs-5%, which contained only Cellulose I.²¹ The formation of a diffraction peak around 12.0° 2θ in TS-CNCs, similarly to the TS cellulose precursors, showed the presence of a small fraction of Cellulose II. However, no formation of allomorphic Cellulose II in CNCs was exhibited in CH cellulose obtained using similar cellulose extraction, as well as acid hydrolysis conditions. The CH-CNCs and CC-CNs showed the typical peaks of only Cellulose I type structure at around 15.0°, 16.0° and 22.0° 2θ .³⁴ The XRD patterns of CNCs from TS, EF, SB and CH, and their cellulose precursors are shown in Figure 1.

Generally, the formation of Cellulose I and II allomorphs in the as-obtained CNCs was dependent on the cellulose source and cellulose extraction conditions, and less influenced by sulfuric acid hydrolysis. From the results, it is

evident that sulfuric acid hydrolysis did not induce complete or partial polymorphic transition of Cellulose I to II in the CNCs isolated, except in TS.

Table 1
Composition of plant materials²⁰ and yields of CNCs with respect to as-extracted cellulose and the untreated by-products

Plant by-products	Composition/yields (%w/w) on dry basis				
	Cellulose	Lignin	Hemicellulose	CNCs from cellulose	CNCs from by-products
TS	36.7 ± 0.55	19.5 ± 1.02	23.6 ± 0.88	56.3 ± 2.45	20.7
EF	60.0 ± 1.25	10.7 ± 0.65	18.5 ± 0.68	54.7 ± 2.54	32.8
SB	39.5 ± 1.08	21.0 ± 0.95	23.4 ± 1.24	42.0 ± 4.21	16.6
CH	35.5 ± 1.80	30.7 ± 0.36	14.8 ± 1.10	30.0 ± 3.56	10.6

Data are presented as the mean ± SD ($n = 3$); (TS – *teff* straw; EF – *enset* fiber; SB – sugarcane bagasse; CH – coffee hull)

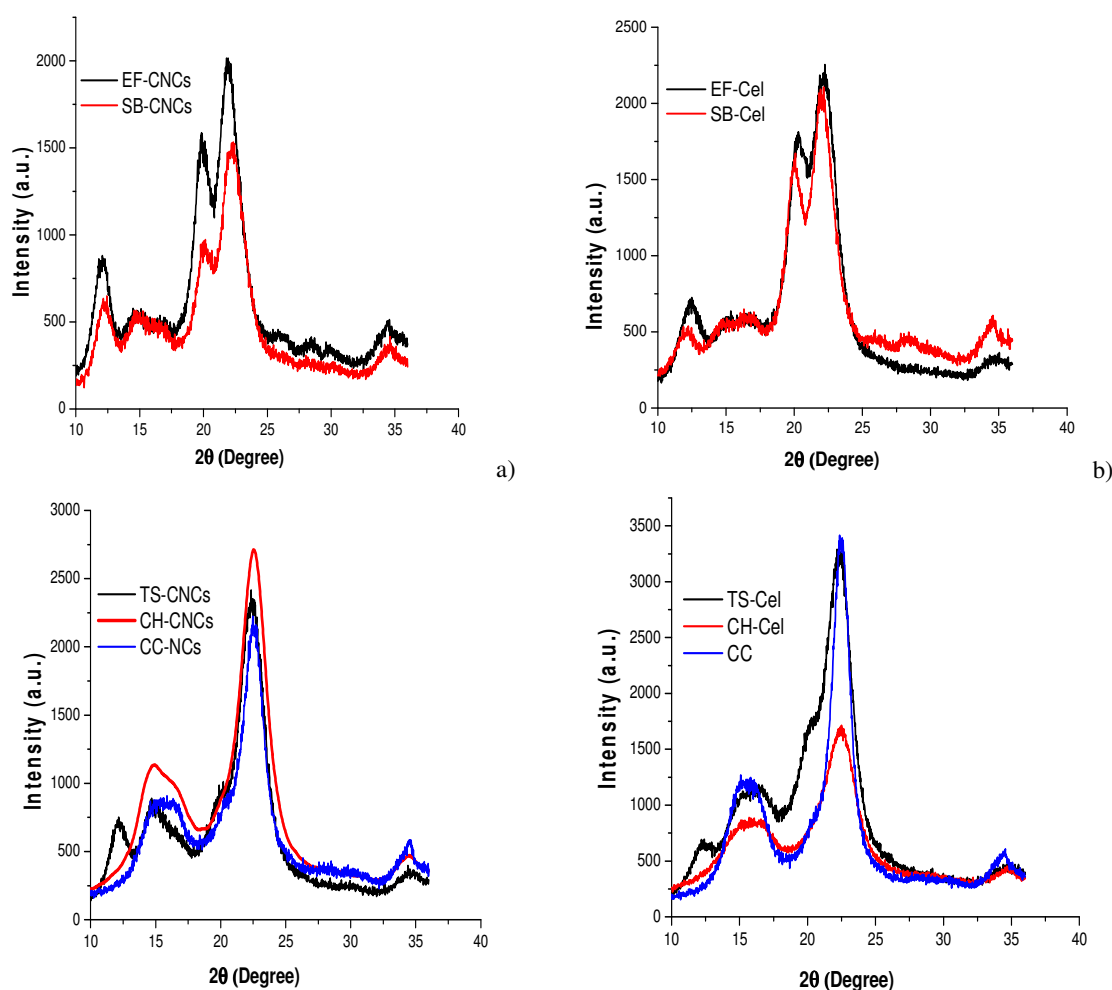


Figure 1: X-ray diffractograms of CNCs of EF and SB (a), and their cellulose precursors (b); and CNCs of TS and CH (c), and their cellulose precursors (d); (CNCs – cellulose nanocrystals; Cel – cellulose; TS – *teff* straw; EF – *enset* fiber; SB – sugarcane bagasse; CH – coffee hull; CC-NCs – cellulose nanocrystals isolated from commercial cellulose (CC) included for comparison)

However, the higher alkaline condition during the process of cellulose extraction, mainly in EF and SB, caused the partial conversion both in as-extracted cellulose and the respective CNCs (Fig. 1). A similar finding was reported in a previous study, where the acid hydrolysis of cellulose did not influence the crystallographic structure of CNCs.³⁵ However, few studies indicate the contribution of sulfuric acid hydrolysis for the formation of Cellulose II or a mixture of Cellulose I and II allomorphs in the CNCs isolated from different sources, such as oil palm microcrystalline cellulose (MCC) I, eucalyptus cellulose I and recycled Tetra Pak packaging cellulose fibers, and *Pongamia pinnata* oil meal.^{10,36–38}

In this study, crystallinity indices (CrIs) were determined following three approaches – those of Segal *et al.*, Hermans *et al.* and Zhang *et al.* (Eqs. 1-3). Higher values of CrI for each material were observed by the Segal *et al.* method.³⁹ Almost equivalent values of CrI were observed in all samples according to the Hermans *et al.* and Zhang *et al.* approaches. For comparison purposes, the method of Segal *et al.* for estimation of CrI is used, which is simple and gives helpful information on the relative degree of crystallinity.^{28,40–42}

From the CNCs containing a considerable fraction of Cellulose II allomorphs, EF-CNCs (76.4%; 56.7%) had higher CrI than SB-CNCs (65.4%; 44.8%), following the Segal *et al.* and Hermans *et al.* approaches, respectively. No drastic decrement of CrIs was recorded in the CNCs of EF and SB when compared to the CrIs of their cellulose precursors. Other studies also reported (slight) reduction of crystallinity of as-obtained CNCs,^{37,43} which could be caused by partial degradation of the crystalline regions.⁴⁴ However, the CrIs of CNCs-I isolated from CH containing only Cellulose I, and TS-CNCs showed an increment, which could be due to the hydrolytic scission of the glycosidic bonds releasing individual crystals and removing the amorphous domains only.⁴⁵

Thus, cellulose extraction under higher alkaline conditions resulted in both partial polymorphic transition from Cellulose I to Cellulose II in the native cellulose and the respective CNCs isolated from TS, EF and SB. Furthermore, lower CrIs of CNCs obtained from EF and SB were recorded, as compared to CNCs isolated from cellulose fibers extracted under

lower alkaline conditions (5% and 10% NaOH).²¹ Generally, CrI continuously decreases in the CNCs with an increase in alkali concentration used in the treatment.¹¹

Table 2 shows different parameters obtained from the (deconvoluted) XRD of CNCs and their cellulose precursors, such as CrIs by the three approaches, d-spacings, crystallite sizes at the 200 plane (τ_{200} values), the proportion of crystallite interior chains for the 200 plane (X_{200}), as well as the fractional variation in the plane spacing for the 200 plane ($\Delta d/d_{200}$) and Z-values (Eqs. 8-12). The Cellulose II fraction present in the EF-CNCs (78.9%) was the highest, followed by SB-CNCs (63.4%), TS-CNCs (41.9%), and CH-CNCs (0%), when considering the intensities at the diffraction lattices of 200 and 110 around 22 and 20° 2 θ , respectively. Moreover, the percentages of the Cellulose II form in the crystalline aggregation and the cellulose samples were estimated employing the equations described elsewhere (Eqs. 4-7).²⁴ The highest Cellulose II form was found in EF-CNCs (62.1%, 35.6%) in the crystalline aggregation and the samples, respectively, and the Cellulose I in the EF-CNCs was (37.8%, 21.8%), respectively. However, no fraction of Cellulose II was observed in CH-CNCs, which could be due to high lignin content in CH, hindering polymorphic transition even at higher alkaline conditions in the pretreatment stage.²⁰

The d-spacings of the CNCs ranged from 0.599-0.732, 0.449-0.528, 0.394-0.404, and 0.257-0.260 for the lattice planes of 1 $\bar{1}\bar{0}$, 110, 200 and 040, as shown in Table 2. Higher values of d-spacings for the plane of 1 $\bar{1}\bar{0}$, and lower values for 110 lattice plane were recorded for EF-CNCs and SB-CNCs, where partial polymorphic transformation occurred. In a study reported elsewhere, the d-spacings of the 1 $\bar{1}\bar{0}$, 110, 200 lattice planes for cellulose I are 0.601 \pm 0.06, 0.535 \pm 0.05 and 0.392 \pm 0.02, respectively. These values shifted to 0.741 \pm 0.06, 4.43 \pm 0.03 and 0.408 \pm 0.04 for Cellulose II.¹¹ The τ_{200} values of CNCs from the four plant sources ranged from 3.86-4.09 nm, and X_{200} and $\Delta d/d_{(200)}$ ranged from 0.496-0.520; 0.0917-0.0980, respectively. There is an inverse relationship between CrIs and $\Delta d/d_{(200)}$ of the CNCs (Table 2). Hydroxide ions penetrate easily into the matrix and therefore shift the concentration required for polymorphic transformation of CNC to a lower value and within a narrower range.¹¹ The negative

numbers of the Z-values in the CNCs isolated from CH indicate that no complete or partial polymorphic transformation happened,^{46,47} as shown in Table 2 and in the XRD patterns (Fig. 1).

Chemical functionality studies

As seen in Figure 2, the bands in the region around 3333 cm^{-1} represent the stretching vibration of the OH groups of cellulose in the CNCs and cellulose precursors. The transmittance bands around $2988\text{--}2900\text{ cm}^{-1}$ correspond to the CH stretching of methyl and methylene groups in cellulose,^{28,45} but intensified in the CNCs and celluloses extracted from TS and EF at higher alkaline conditions, with formation of double bands in the same region.⁴⁴ The band around 1642 cm^{-1} is due to the adsorbed water in the CNCs as well as cellulose precursors. The bands around 1473 and 1380 cm^{-1} reflect CH symmetric and asymmetric deformations, respectively. The absorbance at 1327 cm^{-1} is attributed to the CC and CO skeletal vibrations.⁴⁸ The relative increase in the intensity of the band near 895 cm^{-1} (C1 group frequency) in CNCs obtained at lower acid hydrolysis time indicates the coexistent of Cellulose II.¹⁰

In studies by Oh and others,^{49,50} most FTIR bands, including those at 2901 , 1431 , 1282 , 1236 , 1202 , 1165 , 1032 , and 897 cm^{-1} , were shifted to higher wavenumbers (by $2\text{--}13\text{ cm}^{-1}$) during transformation of Cellulose I to Cellulose II by mercerization ($15\text{--}20\text{ w/w\% NaOH}$) and carbon dioxide treatment. However, the bands at 3352 ,

1373 and 983 cm^{-1} shifted to lower wavenumbers (by $3\text{--}95\text{ cm}^{-1}$).

The bands observed at $\sim 1160\text{ cm}^{-1}$ and $\sim 1101\text{ cm}^{-1}$ are attributed to the ring CC bending vibration and COC glycoside ether bond of the β -1,4-glycosidic ring linkages between the D-glucose units in cellulose. The absorption in the range of $\sim 1024\text{--}1047\text{ cm}^{-1}$ observed in the spectra of CNCs corresponds to the CH stretching vibration of the cellulose component. The bands at 1061 cm^{-1} refer to CO stretching.⁵¹ The band around 890 cm^{-1} in the spectra of cellulose and the respective CNCs is attributed to the interactions between β -glycosidic C₁H deformation linkages and the glucose units of cellulose.^{28,52}

The appearance of a new small band around 1205 cm^{-1} in the CNCs spectra is related to S=O vibration, and shows the esterification reaction during the acid hydrolysis process.⁴⁵ The acid hydrolysis did not change the cellulose molecular structure in the formation of CNCs, rather intensified a few bands around 2900 , 1370 , 1230 , 1060 and 890 cm^{-1} .^{53,54}

Morphological and dimensional analyses

The morphological studies by TEM showed that all the CNCs obtained from the cellulose fibers extracted from the plant by-products were needle-shaped (Fig. 3). TEM images reveal the acid hydrolysis was effective in isolating CNCs. Relatively clear images were taken for most CNCs when phosphotungstic acid solution was used rather than uranyl acetate (images by uranyl acetate not shown).

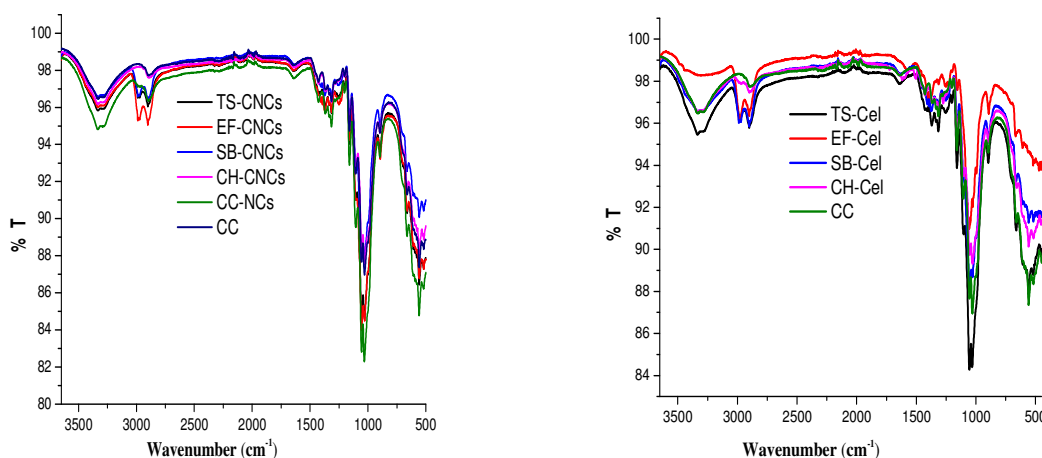


Figure 2: FTIR spectra of CNCs isolated (left), and cellulose precursors (right); (CNCs – cellulose nanocrystals; Cel – cellulose; TS – *teff* straw; EF – *enset* fiber; SB – sugarcane bagasse; CH – coffee hull; CC-NCs – cellulose nanocrystals isolated from commercial cellulose (CC) included for comparison)

Table 2
Parameters obtained from (deconvoluted) XRD of Cellulose II allomorphs in CNCs from TS, EF and SB, and Cellulose I allomorph in CNCs from CH, as well as their cellulose precursors

Materials	d-spacings (nm)				τ_{200} (nm)	X_{200}	$\Delta d/d_{200}$	CrIs (%) according to			Z-Values
	1 $\bar{1}$ 0	110	200	040				Segal <i>et al.</i>	Hermans <i>et al.</i>	Zhang <i>et al.</i>	
TS-CNCs	0.732	0.587	0.396	0.259	3.861	0.497	0.0963	81.21	53.96	60.91	160.76
TS-Cel	0.732	0.563	0.396	0.259	2.935	0.374	0.1269	74.13	59.62	55.60	182.95
EF-CNCs	0.734	0.449	0.404	0.257	3.876	0.498	0.0980	76.42	56.72	57.32	258.83
EF-Cel	0.716	0.560	0.401	0.258	4.091	0.520	0.0920	78.79	59.05	59.09	156.88
SB-CNCs	0.724	0.444	0.399	0.258	4.089	0.520	0.0917	65.43	44.84	49.07	276.33
SB-Cel	0.731	0.547	0.394	0.257	3.881	0.499	0.0954	77.32	55.61	57.99	195.85
CH-CNCs	0.599	0.528	0.394	0.260	3.859	0.496	0.0959	75.67	60.30	56.75	-11.15
CH-Cel	0.613	0.539	0.397	0.261	3.483	0.453	0.1071	66.41	54.10	49.81	2.48
CC-NCs	0.604	0.541	0.394	0.260	4.415	0.550	0.1287	74.91	54.77696248	56.18	-14.18
CC	0.608	0.554	0.395	0.260	6.480	0.679	0.0573	87.23	64.77	65.42	-19.85

(CNCs – cellulose nanocrystals; Cel – cellulose; TS – *teff* straw; EF – *enset* fiber; SB – sugarcane bagasse; CH – coffee hull; CC-NCs – cellulose nanocrystals isolated from commercial cellulose (CC) included for comparison)

The average length, diameter and aspect ratio of the CNCs ranged from 62 to 121 nm, 5.5 to 10.9 nm, 8.95-16.38, respectively (Table 3). In our previous study, higher aspect ratios of CNCs from the four plant samples (17.32-36.68) were recorded when the CNCs were isolated from the cellulose fibers extracted with lower NaOH concentration (5%) in the pretreatment stage.²¹ In

the literature, it was reported that higher alkaline concentration, as well as an increase in the acid hydrolysis time, resulted in a significant decrease in the average length and diameter of the CNCs because of the destruction of amorphous regions and even partial crystalline regions of cellulose.^{6,11,31,42,53}

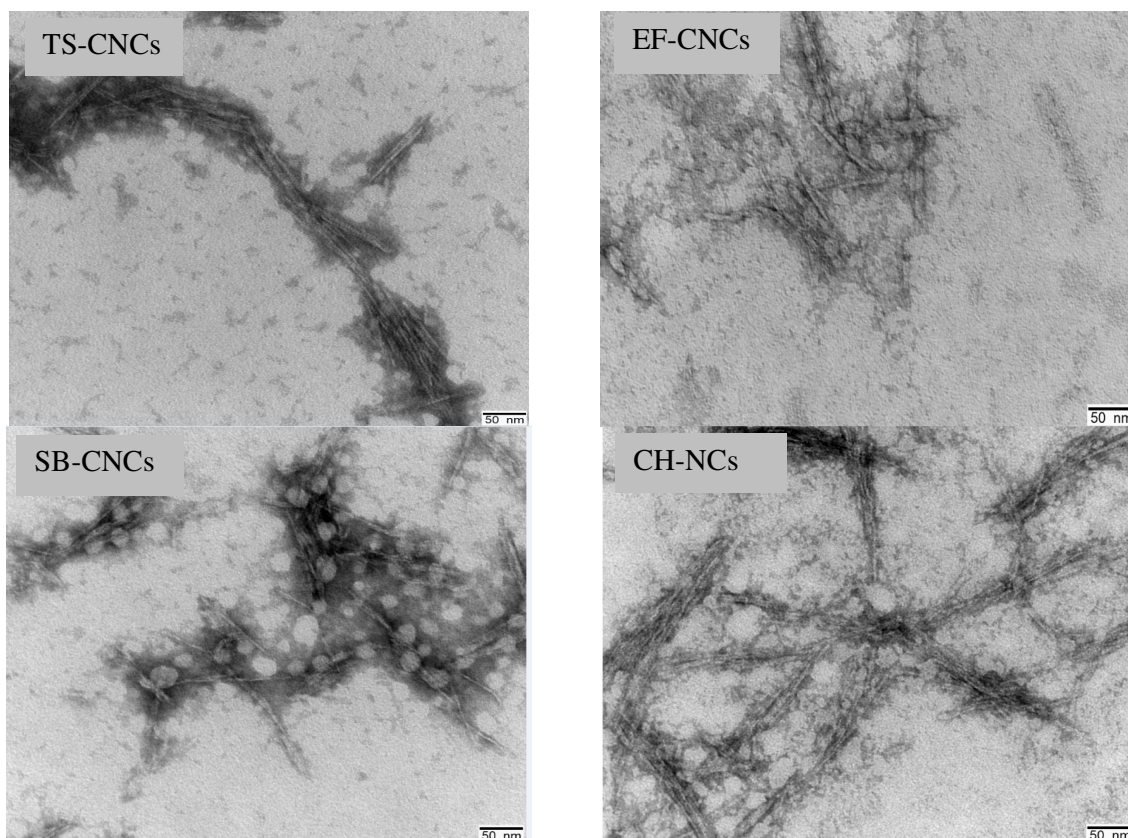


Figure 3: Transmission electron micrographs of CNCs isolated from extracted celluloses (bar scale: 50 nm); (CNCs – cellulose nanocrystals; TS – *teff* straw; EF – *enset* fiber; SB – sugarcane bagasse; CH – coffee hull)

Table 3
TEM dimensional analysis of CNCs isolated from celluloses extracted from various plant byproducts

Source (CNCs)	L_{average} (nm)	Diameter D; D_{average} (nm)	Aspect ratio
TS-CNCs	62.306 ± 13.166	2.5-15.05; 6.82 ± 3.25	9.14
EF-CNCs	89.534 ± 21.401	6.67-18.15; 5.47 ± 1.939	16.38
SB-CNCs	120.59 ± 24.576	6.22-17.46; 10.864 ± 3.21	11.10
CH-CNCs	86.4 ± 17.469	3.54-13.31; 9.651 ± 2.36	8.95

(L_{average} – average length; D_{average} – average diameter of CNCs estimated by ImageJ Software; CNCs – cellulose nanocrystals; TS – *teff* straw; EF – *enset* fiber; SB – sugarcane bagasse; CH – coffee hull)

According to studies reported elsewhere,^{12,35} the Cellulose II of the CNCs had a smaller particle size than Cellulose I of the CNCs, which could be due to partial depolymerization of cellulose chains by mercerization. CNC particles

with short length can be easily obtained when Cellulose I is converted to Cellulose II before sulfuric acid hydrolysis.⁶ Reports indicate that CNCs with high aspect ratios (above 10) exhibit

good mechanical properties (bending strength, tensile strength and Young's modulus).⁵⁵

Thermal properties

Figure 4 displays the thermal degradation characteristics of CNCs isolated, and their cellulose precursors. A clear difference was observed in the TGA and corresponding DTG (Differential Thermo Gravimetry) curves of cellulose and the respective CNCs. The first temperature range between 30-110 °C showed a small weight loss (3.9-5.6%) at T_{max} 59-67 °C, mainly due to water evaporation.⁵⁶ The onset degradation temperature (T_i), the maximum degradation temperature (T_{max}) and maximum weight loss (rate), as well as residue at 550 °C, of the CNCs and cellulose precursors are listed in Table 4.

Two major degradation regions were observed from the DTG curves of all CNCs. The first degradation stage, with a weight loss of 34-38%, occurred in the region at 134-300 °C (T_{max} : 215-

233 °C; (weight loss rate: 0.18-0.21%/°C), which is mainly due to decomposition of sulfate half ester groups and large specific surface area of cellulose chains, when compared to the cellulose precursors (T_{max} : 328-346 °C). The other degradation step was recorded in the region of 277-465 °C (T_{max} : 335-358 °C), with a weight loss of 19-24%, due to breakdown of the interior non-sulfated cellulose crystals.^{10,40,57} As depicted in Figure 4 and Table 4, the reduction in thermal stability was more pronounced for the conversion of cellulose to CNCs rather than the partial polymorphic transition from CNC-I to CNC-II. Such a lower degradation temperature in the CNCs may be attributed to the introduction of the negatively charged sulfate half ester groups and a larger number of free ends of chains in CNCs caused by the sulfuric acid hydrolysis. The thermal degradation behaviors of CNC-I and CNC-II were similar, and the acid hydrolysis had a slight effect on the thermal degradation behaviors of CNC-I and CNC-II, as reported elsewhere.^{6,31}

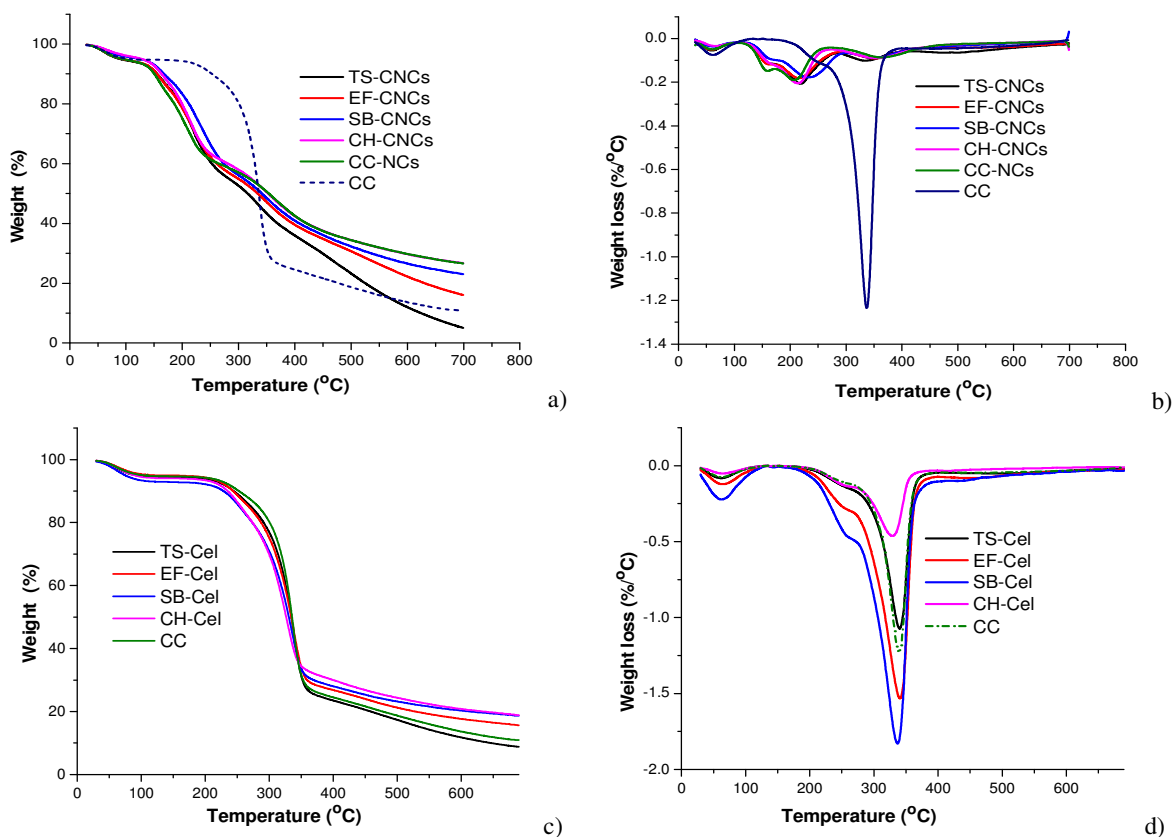


Figure 4: Thermal degradation characteristics of as-isolated CNCs using TGA (a) and DTG (b), and their cellulose precursors using TGA (c) and DTG (d); (CNCs – cellulose nanocrystals; Cel – cellulose; TS – *teff* straw; EF – *en-set* fiber; SB – sugarcane bagasse; CH – coffee hull; CC-NCs – cellulose nanocrystals isolated from commercial cellulose (CC) included for comparison)

Table 4
Summary of thermogravimetric characteristics of TGA and DTG of the CNCs and cellulose precursors

Material	ΔT (°C)	T_{max} (°C)	Weight loss (%)	Weight loss rate (%/°C)	T_i (°C)	Residue at 550 °C (%)
TS-CNCs	29.77-110.22	59.94	5.64	0.0548	134.96	16.99
	134.96-283.58	219.16	38.13	0.2069		
	284.72-413.59	334.80	20.38	0.1012		
TS-Cel	29.70-109.04	61.69	6.25	0.1081	207.15	9.73
	207.15-390.23	342.88	47.52	1.0979		
	390.23-550.00	517.18	14.11	0.0797		
EF-CNCs	29.77-109.56	59.04	5.36	0.0510	133.95	26.36
	133.95-287.37	216.65	36.82	0.1815		
	287.37-418.71	335.76	18.78	0.1011		
EF-Cel	29.99-121.38	65.62	3.15	0.0846	210.43	20.66
	210.43-400.22	346.67	69.04	1.6778		
	400.22-550.00	438.86	5.81	0.0637		
SB-CNCs	29.77-105.07	65.91	3.93	0.0367	139.53	29.12
	139.53-300.39	233.27	37.99	0.1779		
	300.39-433.82	351.61	18.55	0.0884		
SB-Cel	29.72-125.25	57.64	4.85	0.1382	196.76	20.26
	199.76-399.47	340.68	66.59	1.4264		
	399.47-550.00	469.58	7.40	0.0759		
CH-CNCs	29.77-108.21	66.69	3.85	0.0339	134.96	31.86
	134.96-272.07	214.15	33.63	0.2050		
	276.57-464.69	357.53	24.04	0.0893		
CH-Cel	29.77-109.00	56.35	5.48	0.0568	282.45	21.56
	282.45-390.20	327.57	46.24	0.4862		
	390.20-550.00	423.13	9.91	0.0392		
CC-NCs	29.77-108.65	59.94	5.29	0.0495	152.56	31.90
	152.56-171.4	158.6	5.52	0.1484		
	142.00-237.01	206.244	28.60	0.1903		
	286.85-478.15	361.67	22.58	0.0868		
CC	30.16-108.49	62.60	4.70	0.0749	268.93	15.91
	268.93-378.50	338.76	62.20	1.2165		
	378.50-550.00	463.49	9.85	0.0470		

(CNCs – cellulose nanocrystals; Cel – cellulose; TS – *teff* straw; EF – *enset* fiber; SB – sugarcane bagasse; CH – coffee hull; CC-NCs – cellulose nanocrystals isolated from commercial cellulose (CC) included for comparison)

However, a decrease in thermal stability was also exhibited in cellulose fibers or CNCs upon

Enhanced thermal stability was also reported elsewhere,^{38,59} indicating that mercerized samples had better thermal stability properties. All the CNCs exhibited higher char residues at 550 °C than their cellulose counterparts due to a

CONCLUSION

Under higher alkaline conditions, cellulose extraction resulted in partial polymorphic transition of native cellulose of TS, EF and SB and the respective CNCs into Cellulose II. The allomorphic CNCs exhibited reduced CrIs, yield, length and aspect ratios, as compared to CNCs-5%. Morphological and dimensional studies by

polymorphic transition from Cellulose I to Cellulose II.⁵⁸

dehydration effect of the sulfate group as flame retardants.^{10,57,60} Furthermore, the CNCs also showed slightly higher char residues at 550 °C than CNCs-5% reported in our previous work.²¹

TEM revealed formation of needle-shaped nano-scaled particles. TGA revealed two major decomposition processes of the CNCs at T_{max} 215-233 °C and 335-358 °C. In general, the physicochemical properties of the isolated CNCs were dependent on the source of cellulose, cellulose extraction and acid hydrolysis conditions, while the polymorphic transitions were mainly dependent on sources and extraction

conditions of cellulose. Lignocellulosic materials with high lignin content, such as CH, do not easily undergo polymorphic transition even under higher alkaline pretreatment conditions. The higher alkaline condition also resulted in lower degree of crystallinity, crystal size, and aspect ratio. In conclusion, CNCs with Cellulose I and Cellulose II allomorphs can be produced via controlled treatment conditions from plant by-products based on their chemical compositions.

ACKNOWLEDGEMENTS: Addis Ababa University, Ethiopia, is acknowledged for offering the PhD Scholarship to TG. The authors are grateful to Martin Luther University, Germany, for providing access to TEM. Cadila Pharmaceuticals PLC. is acknowledged for providing access to the FTIR spectrophotometer. Adama Science and Technology University, Ethiopia, and Ethiopian Leather Development Institute are acknowledged for access to their X-ray diffractometer and Thermal Analyzer. Tri-Sustain (Economic, Ecological and Therapeutic sustainability) Project in the development of phytopharmaceuticals for Sub-Saharan Africa funded by DAAD (grant number 57369155) and BMBF (grant number 01DG17008B), Germany, as well as Ministry of Innovation and Technology, Ethiopia, partly supported this research work financially.

REFERENCES

- ¹ M. Poletto, H. L. Ornaghi Júnior and A. J. Zattera, *Materials (Basel)*, **7**, 6105 (2014), <https://doi.org/10.3390/ma7096105>
- ² X. F. Sun, R. C. Sun, Y. Su and J. X. Sun, *J. Agric. Food Chem.*, **52**, 839 (2004), <https://doi.org/10.1021/jf0349230>
- ³ C. J. Wijaya, S. N. Saputra, F. E. Soetaredjo, J. N. Putro, C. X. Lin *et al.*, *Carbohydr. Polym.*, **175**, 370 (2017), <https://doi.org/10.1016/j.carbpol.2017.08.004>
- ⁴ E. Durmaz and S. Ateş, *Cellulose Chem. Technol.*, **55**, 755 (2021), <https://doi.org/10.35812/CelluloseChemTechnol.2021.55.63>
- ⁵ A. U. Khan, N. Malik and T. Arfin, in “Nanocellulose and Nanohydrogel Matrices: Biotechnological and Biomedical Applications”, edited by M. Jawaid and F. Mohammad, Wiley-VCH Verlag GmbH & Co. KGaA, Chennai, 2017, pp. 331-353
- ⁶ J. Gong, J. Li, J. Xu, Z. Xiang and L. Mo, *RSC Adv.*, **7**, 33486 (2017), <https://doi.org/10.1039/c7ra06222b>
- ⁷ T. Abitbol, A. Rivkin, Y. Cao, Y. Nevo, E. Abraham *et al.*, *Curr. Opin. Biotechnol.*, **39**, 76 (2016), <https://doi.org/10.1016/j.copbio.2016.01.002>
- ⁸ R. Varma and S. Vasudevan, *Cellulose Chem. Technol.*, **56**, 39 (2022), <https://doi.org/10.35812/cellulosechemtechnol.2022.56.03>
- ⁹ F. I. Ditzel, E. Prestes, B. M. Carvalho, I. M. Demiate and L. A. Pinheiro, *Carbohydr. Polym.*, **157**, 1577 (2017), <https://doi.org/10.1016/j.carbpol.2016.11.036>
- ¹⁰ L. Xing, J. Gu, W. Zhang, D. Tu and C. Hu, *Carbohydr. Polym.*, **192**, 184 (2018), <https://doi.org/10.1016/j.carbpol.2018.03.042>
- ¹¹ E. Jin, J. Guo, F. Yang, Y. Zhu, J. Song *et al.*, *Carbohydr. Polym.*, **143**, 327 (2016), <https://doi.org/10.1016/j.carbpol.2016.01.048>
- ¹² G. Delepierre, S. Eyley, W. Thielemans, C. Weder, E. D. Cranston *et al.*, *Nanoscale*, **12**, 17480 (2020), <https://doi.org/10.1039/d0nr04491a>
- ¹³ B. Minten, S. Tamru, E. Engida and T. Kuma, *Econ. Dev. Cult. Change*, **64**, 265 (2016), <https://doi.org/10.1086/683843>
- ¹⁴ H. Lee, *Open Agric. J.*, **12**, 185 (2018), <https://doi.org/10.2174/1874331501812010185>
- ¹⁵ T. Gebre-Mariam and P. C. Schmidt, *Starch/Staerke*, **48**, 208 (1996), <https://doi.org/10.1002/star.19960480603>
- ¹⁶ H. Berhanu, Z. Kiflie, I. Miranda, A. Lourenço, J. Ferreira *et al.*, *PLoS One*, **13**, 1 (2018), <https://doi.org/10.1371/journal.pone.0199422>
- ¹⁷ D. Bhattacharya, L. T. Germinario and W. T. Winter, *Carbohydr. Polym.*, **73**, 371 (2008), <https://doi.org/10.1016/j.carbpol.2007.12.005>
- ¹⁸ R. C. Alves, F. Rodrigues, M. A. Nunes, A. F. Vinha and M. B. P. P. Oliveira, in “Handbook of Coffee Processing By-Products”, edited by C. M. Galanakis, Academic Press, Elsevier Inc., Chania, Greece, 2017, pp. 1-26, <http://dx.doi.org/10.1016/B978-0-12-811290-8.00001-3>
- ¹⁹ V. Aristizábal-Marulanda, Y. Chacón-Perez and C. A. C. Alzate, in “Handbook of Coffee Processing By-Products”, edited by C. M. Galanakis, Elsevier Inc, Chania, Greece, 2017, pp. 63-86
- ²⁰ T. Gabriel, A. Belete, F. Syrowatka, R. H. H. Neubert and T. Gebre-Mariam, *Int. J. Biol. Macromol.*, **158**, 1248 (2020), <https://doi.org/10.1016/j.ijbiomac.2020.04.264>
- ²¹ T. Gabriel, A. Belete, G. Hause, R. H. H. Neubert and T. Gebre-Mariam, *J. Polym. Environ.*, **29**, 2964 (2021), <https://doi.org/10.1007/s10924-021-02089-3>
- ²² L. Segal, J. J. Creely, A. E. Martin and C. M. Conrad, *Text. Res. J.*, **29**, 786 (1959), <https://doi.org/10.1177/004051755902901003>
- ²³ A. Kljun, T. A. S. Benians, F. Goubet, F. Meulewaeter, J. P. Knox *et al.*, *Biomacromolecules*, **12**, 4121 (2011), <https://doi.org/10.1021/bm201176m>
- ²⁴ J. Zhang, D. Li, X. Zhang and Y. Shi, *J. Appl. Polym. Sci.*, **49**, 741 (1993), <https://doi.org/10.1002/app.1993.070490420>
- ²⁵ P. Mansikkamäki, M. Lahtinen and K. Rissanen,

- Carbohydr. Polym.*, **68**, 35 (2007), <https://doi.org/10.1016/j.carbpol.2006.07.010>
- ²⁶ B. G. Rånby, *Acta Chem. Scand.*, **6**, 116 (1952)
- ²⁷ M. Popescu, C. Popescu, G. Lisa and Y. Sakata, *J. Mol. Struct.*, **988**, 65 (2011), <https://doi.org/10.1016/j.molstruct.2010.12.004>
- ²⁸ M. G. Aguayo, A. F. Pérez, G. Reyes, C. Oviedo, W. Gacitúa *et al.*, *Polymers (Basel)*, **10**, 1145 (2018), <https://doi.org/10.3390/polym10101145>
- ²⁹ M. Matsuo, K. Umemura and S. Kawai, *J. Wood Sci.*, **58**, 113 (2012), <https://doi.org/10.1007/s10086-011-1235-5>
- ³⁰ E. B. Heggset, G. Chinga-Carrasco and K. Syverud, *Carbohydr. Polym.*, **157**, 114 (2017), <https://doi.org/10.1016/j.carbpol.2016.09.077>
- ³¹ J. Gong, L. Mo and J. Li, *Carbohydr. Polym.*, **195**, 18 (2018), <https://doi.org/10.1016/j.carbpol.2018.04.039>
- ³² S. Ahmadzadeh, A. Nasirpour, M. B. Harchegani, N. Hamdami and J. Keramat, *Carbohydr. Polym.*, **188**, 188 (2018), <https://doi.org/10.1016/j.carbpol.2018.01.109>
- ³³ D. Ahuja, A. Kaushik and M. Singh, *Int. J. Biol. Macromol.*, **107**, 1294 (2018), <https://doi.org/10.1016/j.ijbiomac.2017.09.107>
- ³⁴ Z. Hu, X. Cao, D. Guo, Y. Xu, P. Wu *et al.*, *Cellulose Chem. Technol.*, **55**, 501 (2021), <https://doi.org/10.35812/CelluloseChemTechnol.2021.55.45>
- ³⁵ S. Borysiak and A. Grzabka-Zasadzińska, *J. Appl. Polym. Sci.*, **133**, 1 (2016), <https://doi.org/10.1002/app.42864>
- ³⁶ W. P. Flauzino Neto, J. L. Putaux, M. Mariano, Y. Ogawa, H. Otaguro *et al.*, *RSC Adv.*, **6**, 76017 (2016), <https://doi.org/10.1039/c6ra16295a>
- ³⁷ M. K. M. Haafiz, A. Hassan, Z. Zakaria and I. M. Inuwa, *Carbohydr. Polym.*, **103**, 119 (2014), <https://doi.org/10.1016/j.carbpol.2013.11.055>
- ³⁸ D. Nataraj, C. Hu and N. Reddy, *Cellulose Chem. Technol.*, **56**, 29 (2022), <https://doi.org/10.35812/cellulosechemtechnol.2022.56.02>
- ³⁹ S. Park, J. O. Baker, M. E. Himmel, P. A. Parilla and D. K. Johnson, *Biotechnol. Biofuels*, **3**, 1 (2010), <https://doi.org/10.1186/1754-6834-3-10>
- ⁴⁰ K. S. Prado and M. A. S. Spinacé, *Int. J. Biol. Macromol.*, **122**, 410 (2019), <https://doi.org/10.1016/j.ijbiomac.2018.10.187>
- ⁴¹ S. Naduparambath and E. Purushothaman, *Cellulose*, **23**, 1803 (2016), <https://doi.org/10.1007/s10570-016-0904-3>
- ⁴² T. Taflick, L. A. Schwendler, S. M. L. Rosa, C. I. D. Bica and S. M. B. Nachtigall, *Int. J. Biol. Macromol.*, **101**, 553 (2017), <https://doi.org/10.1016/j.ijbiomac.2017.03.076>
- ⁴³ V. F. Korolovych, V. Cherpak, D. Nepal, A. Ng, N. R. Shaikh *et al.*, *Polymer (Guildf)*, **145**, 334 (2018), <https://doi.org/10.1016/j.polymer.2018.04.064>
- ⁴⁴ S. Ventura-Cruz and A. Tecante, *Carbohydr. Polym.*, **220**, 53 (2019), <https://doi.org/10.1016/j.carbpol.2019.05.053>
- ⁴⁵ D. García-García, R. Balart, J. Lopez-Martinez, M. Ek and R. Moriana, *Cellulose*, **25**, 2925 (2018), <https://doi.org/10.1007/s10570-018-1760-0>
- ⁴⁶ U. J. Kim, S. H. Eom and M. Wada, *Polym. Degrad. Stab.*, **95**, 778 (2010), <https://doi.org/10.1016/j.polymdegradstab.2010.02.009>
- ⁴⁷ M. Poletto, A. J. Zattera, M. M. C. Forte and R. M. C. Santana, *Bioresour. Technol.*, **109**, 148 (2012), <https://doi.org/10.1016/j.biortech.2011.11.122>
- ⁴⁸ X. F. Sun, F. Xu, R. C. Sun, P. Fowler and M. S. Baird, *Carbohydr. Res.*, **340**, 97 (2005), <https://doi.org/10.1016/j.carres.2004.10.022>
- ⁴⁹ S. Y. Oh, I. Y. Dong, Y. Shin, C. K. Hwan, Y. K. Hak *et al.*, *Carbohydr. Res.*, **340**, 2376 (2005), <https://doi.org/10.1016/j.carres.2005.08.007>
- ⁵⁰ S. Y. Oh, D. Il Yoo, Y. Shin and G. Seo, *Carbohydr. Res.*, **340**, 417 (2005), <https://doi.org/10.1016/j.carres.2004.11.027>
- ⁵¹ M. Smyth, A. García, C. Rader, E. J. Foster and J. Bras, *Ind. Crop. Prod.*, **108**, 257 (2017), <https://doi.org/10.1016/j.indcrop.2017.06.006>
- ⁵² Z. Wang, Z. Yao, J. Zhou, M. He, Q. Jiang *et al.*, *Int. J. Biol. Macromol.*, **129**, 1081 (2019), <https://doi.org/10.1016/j.ijbiomac.2018.07.055>
- ⁵³ Y. Xiao, Y. Liu, X. Wang, M. Li, H. Lei *et al.*, *Int. J. Biol. Macromol.*, **140**, 225 (2019), <https://doi.org/10.1016/j.ijbiomac.2019.08.160>
- ⁵⁴ A. Gao, H. Chen, J. Tang, K. Xie and A. Hou, *Ind. Crop. Prod.*, **152**, 112524 (2020), <https://doi.org/10.1016/j.indcrop.2020.112524>
- ⁵⁵ F. V. Ferreira, M. Mariano, S. C. Rabelo, R. F. Gouveia and L. M. F. Lona, *Appl. Surf. Sci.*, **436**, 1113 (2018), <https://doi.org/10.1016/j.apsusc.2017.12.137>
- ⁵⁶ F. Hemmati, S. M. Jafari and R. A. Taheri, *Int. J. Biol. Macromol.*, **137**, 374 (2019), <https://doi.org/10.1016/j.ijbiomac.2019.06.241>
- ⁵⁷ H. A. Silvério, W. P. Flauzino Neto, N. O. Dantas and D. Pasquini, *Ind. Crop. Prod.*, **44**, 427 (2013), <https://doi.org/10.1016/j.indcrop.2012.10.014>
- ⁵⁸ D. Ciolacu and V. I. Popa, *Cellulose Chem. Technol.*, **40**, 445 (2006), <https://www.cellulosechemtechnol.ro/>
- ⁵⁹ Y. Yue, Thesis, Louisiana State University LSU Digital Commons, Published online 2011, https://digitalcommons.lsu.edu/gradschool_theses/764
- ⁶⁰ J. W. Rhim, J. P. Reddy and X. Luo, *Cellulose*, **22**, 407 (2015), <https://doi.org/10.1007/s10570-014-0517-7>